## On the thermal behaviour of palladium (II) macrocyclic polycatenars

Francesco Neve[a]; Mauro Ghedini[a]; Oriano Francescangeli[b]

[a] Dipartimento di Chimica, Università della Calabria, Arcavacata di Rende (CS), Italy [b] Dipartimento di Scienze dei Materiali e della Terra, Sezione Fisica Università di Ancona, Ancona, Italy

## PLEASE SCROLL DOWN FOR ARTICLE

# On the thermal behaviour of palladium(II) macrocyclic polycatenars

by FRANCESCO NEVE†*, MAURO GHEDINI† and
ORIANO FRANCESCANGELI‡

†Dipartimento di Chimica, Università della Calabria, I-87030 Arcavacata di Rende
(CS), Italy

‡Dipartimento di Scienze dei Materiali e della Terra, Sezione Fisica Università di
Ancona, Via Brecce Bianche, I-60131 Ancona, Italy

Polycatenar saturated macrocycles 1,10-bis[3,4,5-tris(4-dodecyloxy)benzoyl]-1,10-diaza-4,7,13,16-tetrathiacyclo-octadecane (3b) and 1,10-bis[3,4-bis(4-dodecyloxy)benzoyl]-1,10-diaza-4,7,13,16-tetrathiacyclo-octadecane (3d) reacted with [Pd(MeCN)$_4$][BF$_4$]$_2$ led to the cationic complexes [4b][BF$_4$]$_2$ and [4d][BF$_4$]$_2$, respectively. Complexes [4b][BF$_4$]$_2$ and [4d][BF$_4$]$_2$ showed smectic mesomorphism on heating as confirmed by small angle X-ray diffraction. A concurrent, irreversible structural change of the complex cations was observed and a tentative explanation is suggested.

## 1. Introduction

The general rule that geometric (shape, aspect ratio) and dipolar properties of mesogens determine the symmetry of mesophases has always represented a steady guide in the design of novel thermotropic materials. However, in this respect rather scant attention has been paid to the possibility of building up supramolecular assemblies (which eventually will form fluid phases) through molecules of complementary shape. This principle applies very nicely to the generation of columnar mesophases by means of molecules lacking a canonical disk-like geometry.

Whereas the simplest way to achieve this target was to use polycatenar mesogens [1], more correlated structures were obtained through hydrogen bonding [2–5] or charge transfer [6]. In the case of metallomesogens, dimerization [7] and intermolecular dative interactions [8] were the driving forces. In particular, time-averaged disk-shaped structures can be the result of antiparallel (180° rotation, scheme 1 (a)) or orthogonal (90° rotation, scheme 1 (b)) correlation of nearest neighbours. In the first case, the resulting mesophases have been termed discotic antiphases [8 (b)] by analogy with smectic antiphases [9].

In order to verify whether the orthogonal correlation-approach was a suitable one in the case of ionic macrocyclic metallomesogens, we have synthesized hexacatenar and tetracatenar saturated macrocyclic ligands, studied their complexation behaviour with Pd(II) (scheme 2), and investigated the thermal behaviour of both ligands and complexes, looking for mesomorphic behaviour.

## 2. Experimental

### 2.1. Materials and techniques

All reactions were performed under a dry argon atmosphere in freshly distilled solvents. Anhydrous $N,N$-dimethylacetamide (DMA, Aldrich), 4-(dimethylamino)-pyridine (DMAP, Aldrich), and 1,10-diaza-4,7,13,16-tetrathiacyclo-octadecane (1) (Lancaster) were used as
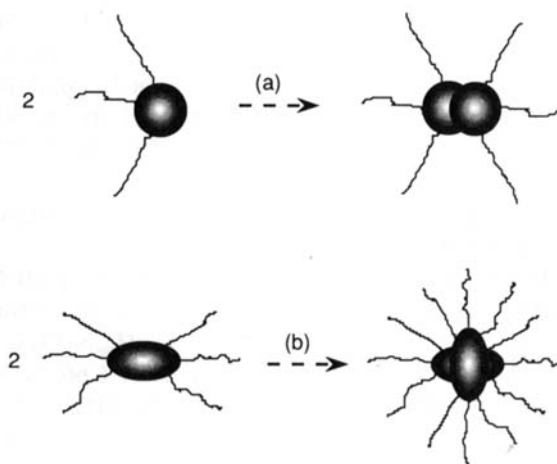


Scheme 1. Examples of correlated mesogenic structures.

*Author for correspondence.

received. [Pd(MeCN)$_4$][BF$_4$]$_2$ was synthesized according to the literature [10].

$^1$H and $^{13}$C NMR spectra were recorded using a Bruker WH 300 spectrometer with SiMe$_4$ as internal reference. IR spectra were recorded using a Perkin-Elmer 2000 FT-IR spectrophotometer. Elemental analyses were performed by the Microanalytical Laboratory of our department.

Optical textures were observed with a Zeiss Axioskop polarizing microscope equipped with a Linkam CO 600 heating stage. Differential scanning calorimetry (DSC) measurements were carried out with a Perkin-Elmer DSC-7 operating at a scanning rate of 10°C min$^{-1}$. X-ray diffraction experiments were carried out as reported earlier [11].

## 2.2. *Synthesis of the ligands*

The synthetic procedure for the preparation of ligands **3b–d** was similar and only a representative example will be given for **3b**.

### 2.2.1. *1,10-Bis[3,4,5-tris(dodecyloxy)benzoyl]-1,10-diaza-4,7,13,16-tetrathiacyclo-octadecane (3b)*

A mixture of macrocycle **1** (0·325 mmol) and benzoyl chloride **2b** (0·712 mmol) in dry DMA (25 ml) in the presence of DMAP (0·712 mmol) was heated with stirring at *c.* 90°C under Ar for 48 h. The mixture was then filtered and the filtrate evaporated to dryness. The residue was redissolved in 50 ml of CHCl$_3$ and washed twice with brine (2 × 25 ml) and water (2 × 25 ml). The organic layer was dried over Na$_2$SO$_4$ (2 h) and rotary evaporated to give a yellowish oil. The pure product was obtained as a waxy white solid in 58% yield after chromatography (silica gel, 1% methanol/CH$_2$Cl$_2$ as eluent). M.p. 79°C. FAB-MS (*m*-NBA, *m/z*) 1639 ([M + H]$^+$). FT-IR (Nujol mull, cm$^{-1}$) 1627 (*v*(CO)). Calc. for C$_{98}$H$_{178}$N$_2$O$_8$S$_4$: C 71·74; H 10·94; N 1·71. Found: C 71·99; H 11·17; N 1·70 per cent. $^1$H NMR (CDCl$_3$, ppm) 0·81 (t, 9H), 1·19–1·39 (m, 54 H), 1·72 (m, 6 H), 2·75 (br, 8 H), 3·60 (br, 4 H), 3·89 (br t, 6 H), 6·51 (s, 2 H, aromatic). $^{13}$C{$^1$H} NMR (CDCl$_3$, ppm) 14·0, 22·6, 26·1, 29·3, 29·4, 29·57, 29·61, 30·3, 31·2(v br), 31·9, 33·1, 48·4(v br), 69·5, 73·5, 105·8, 130·7, 139·7, 153·2, 172·0.

### 2.2.2. *1,10-Bis[3,4,5-tris(methoxy)benzoyl]-1,10-diaza-4,7,13,16-tetrathiacyclo-octadecane (3c)*

Reflux time: 72 h. Yield 82%. M.p. 208°C. FAB-MS (*m*-NBA, *m/z*) 715 ([M + H]$^+$). FT-IR (Nujol mull, cm$^{-1}$) 1627 (*v*(CO)). Calc. for C$_{32}$H$_{46}$N$_2$O$_8$S$_4$: C 53·70; H 6·49; N 3·92. Found: C 53·70; H 6·66; N 3·64 per cent. $^1$H NMR (CDCl$_3$, ppm) 2·84 (br, 8H), 3·67 (br, 4 H), 3·86 (s, 3 H), 3·87 (s, 6 H), 6·64 (s, 2 H, aromatic). $^{13}$C{$^1$H} NMR (CDCl$_3$, ppm) 31·8(v br), 33·8, 48·0(v br), 57·1, 61·5, 105·3, 132·0, 140·3, 154·1, 172·1.

### 2.2.3. *1,10-Bis[3,4-bis(dodecyloxy)benzoyl]-1,10-diaza-4,7,13,16-tetrathiacyclo-octadecane (3d)*

Reflux time: 24 h. Yield 59%. M.p. 101°C. FAB-MS (*m*-NBA, *m/z*) 1271 ([M + H]$^+$). FT-IR (Nujol mull, cm$^{-1}$) 1627 (*v*(CO)). Calc. for C$_{74}$H$_{130}$N$_2$O$_6$S$_4$: C 69·87; H 10·30; N 2·20. Found: C 70·03; H 10·43; N 2·22 per cent. $^1$H NMR (CDCl$_3$, ppm) 0·86 (t, 6H), 1·24–1·44 (m, 36 H), 1·79 (m, 4 H), 2·78 (br, 8 H), 3·65 (br, 4 H), 3·97 (t, 2 H), 3·98 (t, 2H), 6·83 (d, 1 H, aromatic), 6·87 (dd, 1H, aromatic), 6·94 (s, 1H, aromatic). $^{13}$C{$^1$H} NMR (CDCl$_3$, ppm) 14·0, 22·6, 26·0, 29·26, 29·34, 29·6, 31·1(v br), 31·8, 33·1, 48·9(v br), 69·3, 69·6, 113·2, 119·8, 128·5, 149·1, 150·6, 171·9.

## 2.3. *Synthesis of the complexes*

The complexes [**4b–d**][BF$_4$]$_2$ were prepared as described for [**4a**][BF$_4$]$_2$ [12]. The complexes were fully characterized and experimental data are as follows.

### 2.3.1. *[4b][BF$_4$]$_2$*

Yield 65%. FT-IR (Nujol mull, cm$^{-1}$) 1645 (*v*(CO)). Calc. for C$_{74}$H$_{130}$B$_2$F$_8$N$_2$O$_6$PdS$_4$: C 61·28; H 9·34; N 1·46. Found: C 61·18; H 9·46; N 1·30 per cent. $^1$H NMR (CD$_2$Cl$_2$, ppm) 0·88 (t, 9 H), 1·27–1·46 (m, 54 H), 1·72–1·77 (m, 6 H), [3·30 (v br), 3·50 (v br)] (overall integral 8 H), 3·95 (t, 4 H), 4·00 (t, 2H), 4·10 (br, 4 H), 6·71 (s, 2H, aromatic). $^{13}$C{$^1$H} NMR (CD$_2$Cl$_2$, ppm) 13·6, 22·4, 25·9, 26·0, 29·1, 29·27, 29·44, 30·1, 31·7, 37·0(v br), 44·5(v br), 69·3, 73·2, 105·0, 129·3, 139·6, 153·4.

### 2.3.2. *[4c][BF$_4$]$_2$*

Yield 85%. FT-IR (Nujol mull, cm$^{-1}$) 1645 (*v*(CO)). Calc. for C$_{32}$H$_{46}$B$_2$F$_8$N$_2$O$_8$PdS$_4$: C 38·63; H 4·66; N 2·82. Found: C 38·71; H 4·61; N 2·67 per cent. $^1$H NMR (DMSO-$d_6$, ppm) 2·94 (s, 3H), 3·05 (s, 6H), 6·04 (s, 2H, aromatic).

### 2.3.3. *[4d][BF$_4$]$_2$*

Yield 84%. FT-IR (Nujol mull, cm$^{-1}$) 1657, 1635 (*v*(CO)). Calc. for C$_{74}$H$_{130}$B$_2$F$_8$N$_2$O$_6$PdS$_4$: C 57·27; H 8·44; N 1·80. Found: C 57·10; H 8·39; N 2·02 per cent. $^1$H NMR (CD$_3$NO$_2$/CD$_3$CN, ppm) 0·86 (t, 6H), 1·27–1·45 (m, 36 H), 1·77 (m, 4 H), 3·46 (br, 8 H), 3·83 (br, 4 H), 3·98 (t, 2H), 4·03 (t, 2H), 6·98 (d, 1 H, aromatic), 7·09 (s, 1H, aromatic), 7·16 (br d, 1H, aromatic). $^{13}$C{$^1$H} NMR (CD$_3$NO$_2$/CD$_3$CN, ppm) 13·7, 22·0, 22·7, 26·2, 29·0, 29·37, 29·46, 29·7, 32·0, 38·2(v br), 45·6(v br), 69·4, 69·9, 113·0, 113·5, 121·1, 127·0, 149·5, 151·9, 173·9.

## 3. Results and discussion

Direct acylation of macrocycle **1** led to the diamides **3b–d** (scheme 2). Benzoyl chlorides **2b–d** were obtained in a three-steps synthesis following a procedure reported by Malthête [1 (*a*)] and slightly modified by Mertesdorf

2a, $R_1 = R_3 = H$; $R_2 = OC_{12}H_{25}$
2b, $R_1 = R_2 = R_3 = OC_{12}H_{25}$
2c, $R_1 = R_2 = R_3 = OCH_3$
2d, $R_1 = H$; $R_2 = R_3 = OC_{12}H_{25}$

3a-d

4a-d

(i) dry DMA, DMAP, 90 °C
(ii) [Pd(MeCN)$_4$][BF$_4$]$_2$, CH$_2$Cl$_2$, room temperature
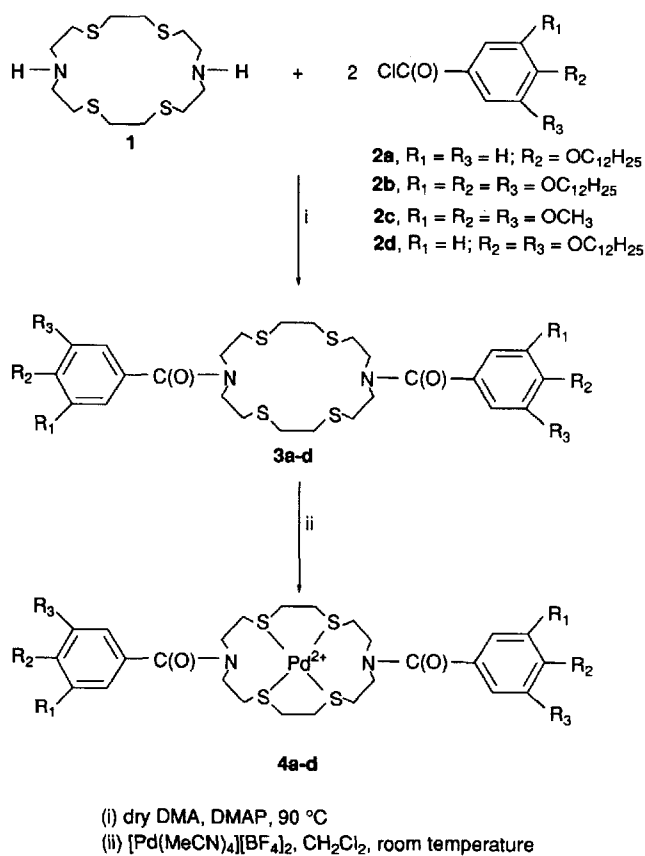
Scheme 2. Synthetic scheme for complexes **4a–d**.

and Ringsdorf [13]. The synthesis of **3a** has been reported previously [12].

Macrocycles **3b–d** were recovered as very soluble (common organic solvents) white solids in good yield (58–82%) and their purity was checked by analytical (elemental analysis, FAB-MS) and spectroscopic methods (IR, $^1$H and $^{13}$C NMR). Compounds **3b** and **3d** were not mesomorphic due to the high conformational freedom of the macrocyclic core [14]. This may have two main consequences: (a) a high flexibility of the macrocyclic ring reduces the length of the rigid core of the molecule; (b) decoupling through flexibility leaves two independent promesogenic units with an individual rigid part too short to support mesomorphism. The melting temperature of **3b** (79°C; $\Delta H = 105 \cdot 5 \,\mathrm{kJ\,mol^{-1}}$) was found to be close to that of **3a** (73°C) which bears only two terminal chain (dodecyloxy) substituents. Therefore going from a roughly rod-like molecule (**3a**) to a polycatenar species (**3b**) has almost no effect on the thermal behaviour. The powder X-ray diffraction (XRD) pattern of **3b** at room temperature is consistent with a lamellar solid with main periodicity $d$ at 44·9 Å. The tetra-branched ligand **3d** showed a higher melting temperature (101°C) and a stronger tendency to super-

cooling. DSC analysis showed that melting on first heating ($\Delta H = 131 \cdot 3 \,\mathrm{kJ\,mol^{-1}}$) was not reversed on cooling (cooling rate $10°\mathrm{C\,min^{-1}}$), and an almost negligible crystallization process ($\Delta H = -3 \cdot 6 \,\mathrm{kJ\,mol^{-1}}$) occurred at 50°C. A second heating/cooling cycle carried out two weeks after the first one allowed us to observe a glass transition at 51°C (midpoint of the change in heat capacity), whereafter melting was observed at 100°C ($\Delta H = 129 \cdot 3 \,\mathrm{kJ\,mol^{-1}}$). Diffraction experiments confirmed this behaviour, as well as the lamellar nature of the solid ($d = 45 \cdot 8$ Å).

Ligand **3b**, although not mesomorphic, may be a good candidate to generate a branched, more rigid mesogen upon coordination of a transition metal ion. The $S_4$ donor set is suitable for square planar coordination of Pd(II) [12, 15] and the six alkoxy chains on the periphery may provide the necessary hydrocarbon content. Planar coordination should not dramatically modify the shape of **3b**, whose 'planar' conformation (with all-*trans*, extended chains) is shown in figure 1. *Endo* metal coordination would also prevent the collapse of the macrocyclic cavity.

Reaction of [Pd(MeCN)$_4$][BF$_4$]$_2$ with **3b** in dichloromethane led to [**4b**][BF$_4$]$_2$, obtained as a pale yellow solid insoluble in most organic solvents. A dilute solution of [**4b**][BF$_4$]$_2$ in CD$_2$Cl$_2$ revealed broad NMR signals both in the proton and carbon-13 spectra. Spectroscopic data were however sufficient to exclude the presence of more than one reaction product.

The thermal behaviour of [**4b**][BF$_4$]$_2$ indicated the presence of a transient mesophase. The melting process took place very slowly upon heating a virgin sample above 160°C as observed by polarizing optical microscopy. Within 20 min the crystalline solid softened first, then gave rise to a highly viscous phase which was already established at 165°C (figure 2). Pressing the coverslip induced flow of the birefringent areas and further heating increased the birefringence of the phase up to 175°C. Above this temperature, the brightness diminished and isotropic areas increased in size. Noticeably, the melting process was accompanied by an irreversible colour change from pale yellow to golden yellow then orange. The melt cleared at around 190°C. The DSC thermograph of the heating cycle of [**4b**][BF$_4$]$_2$ encompassed a single broad peak centred at 188°C, with a shoulder between 153 and 180°C (overall $\Delta H = 92 \cdot 9 \,\mathrm{kJ\,mol^{-1}}$). Once the melt entered the isotropic state it was not possible to recover either the mesophase or the pristine solid phase by cooling. There was obtained only a glassy, indefinitely stable, orange solid, which did not show mesomorphic properties on subsequent heating.

XRD experiments supported the smectic character of the transient mesophase. Figure 3 shows the powder XRD patterns of [**4b**][BF$_4$]$_2$ recorded at different
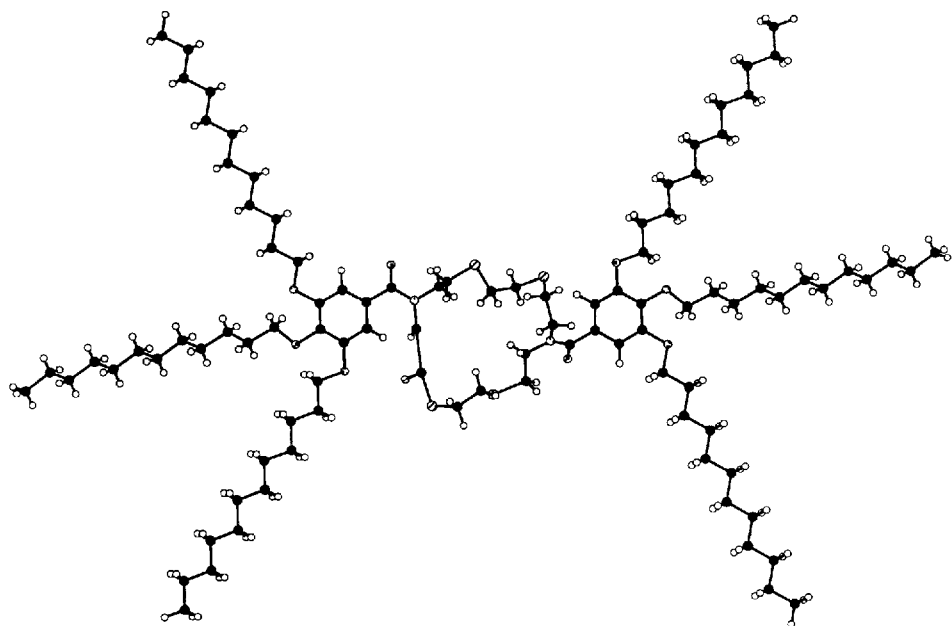
Figure 1.  Molecular   model   of
    ligand **3b** with fully extended,
    all-*anti* chains.

temperatures during the first heating cycle. The lamellar
structure of the room temperature (RT) solid phase of
this sample is apparent, although the quality of the
crystalline structure is rather poor. Very few reflections
are observed throughout the whole spectrum, and those
located in the wide angle region have a rather diffuse
character. In addition, the lowest angle diffraction peak
($d = 40\cdot6$ Å) is largely dominant and the next four peaks
in the region $2\theta < 12°$ are its first four harmonics. The
above diffraction pattern remained essentially unaffected
until the melting temperature ($T \approx 165°C$) was reached.
Only a slight reduction of the layer spacing $d$ was
observed with increasing temperature (figure 4, open
squares) accompanied by a broadening of the wide-angle
signal centred at about $2q = 20°$. This latter evidence
indicates a progressive loss of lateral correlation among
the molecular segments within the layers as the temper-
ature increased. At 170°C the diffraction pattern features
three sharp reflections whose spacings are in the ratio
$1:2:4$ (the third harmonic being too weak to be
detected) and a wide-angle diffuse signal at about $4\cdot5$ Å.
The main layer spacing at 170°C was $37\cdot9$ Å. The above
spectrum is characteristic of a lamellar mesophase with
no order within the layers (consistent with a disordered
smectic mesophase). This mesophase persisted up to the
clearing point with a continuous reduction of the longit-
udinal layer correlation. On cooling from the isotropic
melt, the spectrum of an isotropic glass was observed.
No crystallization of the sample occurred even after
prolonged annealing (about 30 days) at room temper-
ature. Since we had neither precise information on the
molecular structure of $[4b][BF_4]_2$ (crystal growth was

not successful due to either low solubility or poor
tendency to crystallization) nor was it possible to clarify
the nature of 'melted $[4b][BF_4]_2$', we resolved to
synthesize a lower homologue, only for crystallo-
graphic purposes. Ligand **3c**, the methoxy homologue
of **3b**, readily replaced the acetonitrile ligands in
$[Pd(MeCN)_4][BF_4]_2$ to give $[4c][BF_4]_2$. Unfortun-
ately, $[4c][BF_4]_2$ was even less soluble than $[4b][BF_4]_2$
and, more important, it did not melt, decomposing
above 250°C.

The tetracatenar **3d** was then complexed to Pd(II)
leading to $[4d][BF_4]_2$ as a pale yellow solid. A pristine
sample of $[4d][BF_4]_2$ showed a phase behaviour rather
different from that of $[4b][BF_4]_2$, although both melting
and isotropization temperatures were similar. Several
transitions were observed by DSC during the first heating;
these did not always correspond to major visible changes
by polarized light microscopy. DSC peaks were at 73 and
80°C (overall $\Delta H = 33\cdot2$ kJ mol$^{-1}$), 96°C ($\Delta H =$
$46\cdot4$ kJ mol$^{-1}$), and 196°C ($\Delta H = 57\cdot4$ kJ mol$^{-1}$). A very
viscous birefringent phase began to form after annealing
for 10 min at 165°C. The phase was well established above
170°C and birefringence persisted when the cover slip
was pressed. Clearing to an orange isotropic liquid was
seen at 198°C. On cooling, an isotropic glass was usually
observed, although occasionally incomplete formation of
a glassy mesophase was observed in the form of birefrin-
gent domains over a dark background. Neither the
appearance of the mesophase nor crystallization on cool-
ing was however detected by X-ray diffraction.

Figure 5 shows the dependence of the XRD patterns
of $[4d][BF_4]_2$ on temperature. The RT pattern is typical
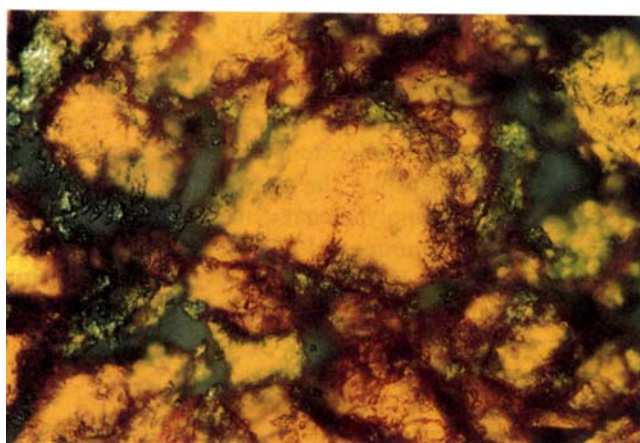
(a)
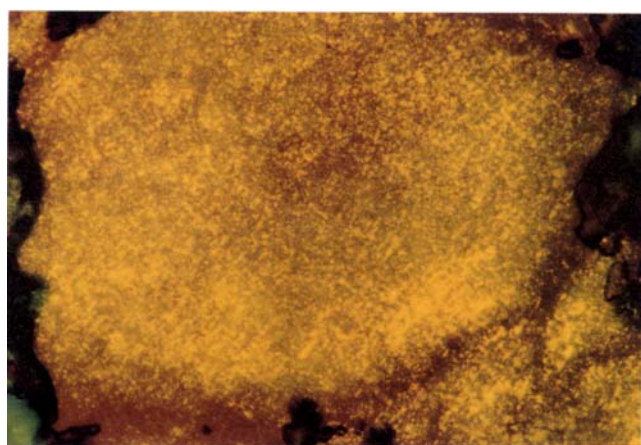


(b)

Figure 2. Polarizing micrographs of [**4b**][BF$_4$]$_2$ taken during the first heating run (*a*) after 15 min at 165°C; (*b*) after shearing the coverslip at 175°C.
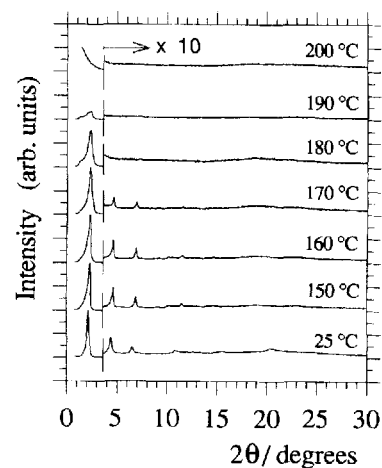


Figure 3. Powder XRD patterns of [**4b**][BF$_4$]$_2$ recorded as a function of temperature (first heating run).



Figure 4. Temperature dependence of the *d* spacing in the first heating cycle for [**4b**][BF$_4$]$_2$ (open squares) and [**4d**][BF$_4$]$_2$ (full circles).

of a highly crystalline phase Cr$_1$ with a pronounced lamellar structure. The spacing corresponding to the dominant diffraction peak is at 26·5 Å. The same pattern was observed with increasing temperature up to 75°C. A further increase in the temperature produced a continuous modification of the diffraction pattern up to 100°C, whereupon a second crystalline phase Cr$_2$ (*d* = 29·6 Å) stabilized itself. A comparison between the spectra of Cr$_1$ and Cr$_2$ shows that in Cr$_2$, formation of a stronger lamellar structure is accompanied by a reduction in the quality of the crystalline structure. The Cr$_2$ phase was stable up to 160°C. At *T* ≈ 165°C a phase transition to a lamellar mesophase with no order in the layers took place. The corresponding spectrum at *T* = 170°C was characterized by one sharp low angle reflection (*d* = 42·1 Å) and a wide angle diffuse halo at



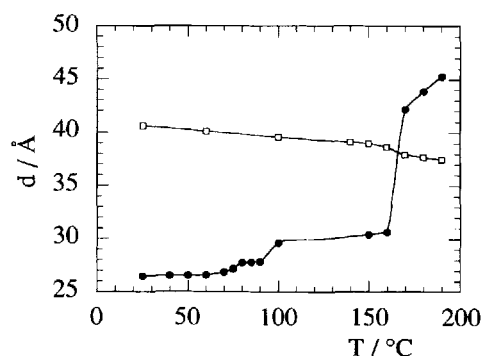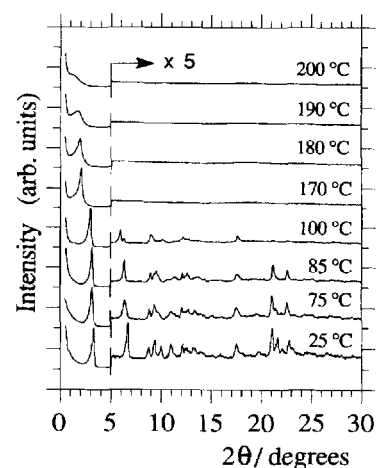Figure 5. Powder XRD patterns of [**4d**][BF$_4$]$_2$ recorded as a function of temperature (first heating run).

about 4·5 Å. A continuous increase of the width of the low angle Bragg peak was observed with increasing temperature over the range of existence of the mesophase (figure 4, full circles); this is consistent with a reduction in the longitudinal coherence length of the layers. On cooling from the isotropic melt, a spectrum very similar to that of the isotropic phase was observed, and this remained essentially unaffected throughout the whole temperature range down to RT.

## 4. Conclusions

The results presented above are not very satisfying with respect to the desired formation of correlated superstructures, although the induction of smectic mesophases has been clearly demonstrated for the tetrafluoroborate salts of $[4b]^{2+}$ and $[4d]^{2+}$. The formation of the mesophase is a rather slow process and seems to be related to a substantial change in the coordinative environment of the palladium centres. Whereas we have no evidence of metal reduction or dissociation, other points must be considered or at least not disregarded. The irreversible change on heating is associated (for a sample taken to the isotropic state and then quenched to room temperature) with: ($i$) an increased solubility in polar solvents; ($ii$) minor changes in the IR spectrum, except for a new absorption of medium intensity occurring at 1715–1720 cm$^{-1}$; ($iii$) proton NMR signals for the hydrogen atoms of the macrocyclic ring consistent with a non-fluxional structure with reduced symmetry. In principle the tetracoordinated palladium(II) ion can still increase its coordination number, although the only accessible donor atoms would be either an O(amide) or an N(amide). N-coordination of an amide is very rare [16], but it may explain the presence of a new carbonyl stretching with ketonic character. We are aware that this tentative explanation is rather weak and further evidence is needed to support it.

All the observed changes, points ($i$)–($iii$), were similar for both the $[4b]^{2+}$ and $[4d]^{2+}$ complexes†. We believe that at the melting temperature a conformational change slowly takes place, which enables a mesophase to develop. This change may also be concurrent with a significant shape reorganization (at least in the case of $[4d]^{2+}$). It is noteworthy that no similar changes have been observed for silver(I) derivatives of the same ligands [17], thus confirming the peculiar behaviour of palladium(II) species. Once in the isotropic state, the disorder of the aliphatic chains might be too high to allow the system to recover any degree of order upon

cooling. A strong tendency to give glassy mesophases has been recently observed for cationic silver(I) mesogens [18, 19] and this tendency seems to increase with the number of peripheral aliphatic chains.

In conclusion, the polycatenar cationic complexes of this study failed to display the mesomorphic polymorphism typical of polycatenar mesogens [1, 6, 19]. Regardless of the number of chains, only a disordered smectic phase was observed. Moreover, the formation of the mesophase is not a reversible process and this limits further investigation.

## References

[1] (a) MALTHÊTE, J., LEVELUT, A.-M., and NGUYEN, H. T., 1985, *J. Phys. Lett., Paris*, **46**, L-875; (b) MALTHÊTE, J., NGUYEN, H. T., and DESTRADE, C., 1993, *Liq. Cryst.*, **13**, 2.

[2] BRIENNE, M.-J., GABARD, J., LEHN, J. M., and STIBOR, I., 1989, *J. chem. Soc. chem. Commun.*, 1868.

[3] MALTHÊTE, J., LEVELUT, A.-M., and LIEBERT, L., 1992, *Adv. Mater.*, **4**, 37.

[4] KLEPPINGER, R., LILLYA, C. P., and YANG, C., 1995, *Angew. Chem. Int. Ed. Engl.*, **34**, 1637.

[5] PALEOS, C. M., and TSIOURVAS, D., 1995, *Angew. Chem. Int. Ed. Engl.*, **34**, 1696.

[6] NUTZ, U., DIELE, S., PELZL, G., RINGSDORF, H., PAULUS, W., and WILSON, G., 1995, *Liq. Cryst.*, **18**, 699.

[7] (a) BARBERA, J., CATIVIELA, C., SERRANO, J. L., and ZURBANO, M. M., 1991, *Adv. Mater.*, **3**, 602; (b) ATENCIO, R., BARBERA, J., CATIVIELA, C., LAHOZ, F. J., SERRANO, J. L., and ZURBANO, M. M., 1994, *J. Am. chem. Soc.*, **116**, 11558.

[8] (a) LAI, C. K., SERRETTE, A. G., and SWAGER, T. M., 1992, *J. Am. chem. Soc.*, **114**, 7948; (b) ZHENG, H., LAI, C. K., and SWAGER, T. M., 1994, *Chem. Mater.*, **6**, 101; (c) SERRETTE, A. G., and SWAGER, T. M., 1994, *Angew. Chem. Int. Ed. Engl.*, **33**, 2342; (d) SERRETTE, A. G., LAI, C. K., and SWAGER, T. M., 1994, *Chem. Mater.*, **6**, 2252.

[9] PROST, J., 1984, *Adv. Phys.*, **33**, 1.

[10] THOMAS, R. R., and SEN, A., 1990, *Inorg. Synth.*, **28**, 63.

[11] NEVE, F., GHEDINI, M., LEVELUT, A.-M., and FRANCESCANGELI, O., 1994, *Chem. Mater.*, **6**, 70.

[12] NEVE, F., and GHEDINI, M., 1993, *J. Inclus. Phenom.*, **15**, 259.

[13] MERTERSDORF, C., and RINGSDORF, H., 1989, *Liq. Cryst.*, **5**, 1757.

[14] (a) TUFFIN, R. P., TOYNE, K. J., GOODBY, J. W., 1995, *J. Mater. Chem.*, **5**, 2093; (b) BLAKE, A. J., BRUCE, D. W., FALLIS, I. A., PARSONS, S., RICHTZENHAIN, H., ROSS, S. A., and SCHRÖDER, M., 1996, *Phil. Trans. R. Soc. Lond. A*, **354**, 395.

[15] REID, G., BLAKE, A. J., HYDE, T. I., and SCHRÖDER, M., 1988, *J. chem. Soc. chem. Commun.*, 1397.

[16] LEE, J. C., JR., MULLER, B., PREGOSIN, P., YAP, G. P. A., RHEINGOLD, A. L., and CRABTREE, R. H., 1995, *Inorg. Chem.*, **34**, 6295.

[17] NEVE, F., unpublished results.

[18] NEVE, F., GHEDINI, M., and FRANCESCANGELI, O., 1995, *J. Mater. Chem.*, **5**, 931.

[19] BRUCE, D. W., DONNIO, B., GUILLON, D., HEINRICH, B., and IBN-ELHAJ, M., 1995, *Liq. Cryst.*, **19**, 537.

†In this light, a reinvestigation of the thermal behaviour of $[4a][BF_4]_2$ gave similar results.